HHS Public Access

Author manuscript

Cell Calcium. Author manuscript; available in PMC 2023 January 01.

Published in final edited form as:

Cell Calcium. 2022 January ; 101: 102519. doi:10.1016/j.ceca.2021.102519.

Structural biology of cation channels important for lysosomal calcium release

Ninghai Gan[1,2,3], **Youxing Jiang**[1,2,3]

[1]Department of Physiology, University of Texas Southwestern Medical Center, Dallas, Texas 75390, USA

[2]Department of Biophysics, University of Texas Southwestern Medical Center, Dallas, Texas 75390 USA

[3]Howard Hughes Medical Institute, University of Texas Southwestern Medical Center, Dallas, Texas 75390 USA

Abstract

Calcium is one of the most important second messengers in cells. The uptake and release of calcium ions are conducted by channels and transporters. Inside a eukaryotic cell, calcium is stored in intracellular organelles including the endoplasmic reticulum (ER), mitochondrion, and lysosome. Lysosomes are acid membrane-bounded organelles serving as the crucial degradation and recycling center of the cell. Lysosomes involve in multiple important signaling events, including nutrient sensing, lipid metabolism, and trafficking. Hitherto, two lysosomal cation channel families have been suggested to function as calcium release channels, namely the Two-pore Channel (TPC) family, and the Transient Receptor Potential Channel Mucolipin (TRPML) family. Additionally, a few plasma membrane calcium channels have also been found in the lysosomal membrane under certain circumstances. In this review, we will discuss the structural mechanism of the cation channels that may be important for lysosomal calcium release, primarily focusing on the TPCs and TRPMLs.

1. Introduction

Ca^{2+} is an important second messenger in cells that regulates many central cellular activities, including cell mobility, enzyme activity, ion channel regulation, and gene expression[1-4]. The cytosolic Ca^{2+} concentration is around 100 nM under resting conditions, which is thousands of fold lower than that of the extracellular environment[1]. The intracellular concentration of Ca^{2+} is tightly regulated by various mechanisms, including its storage inside and release from intracellular organelles such as the endoplasmic reticulum (ER), mitochondrion, and lysosome[5]. Nicotinic acid adenine dinucleotide phosphate (NAADP), inositol 1,4,5-trisphosphate (IP3), and cyclic adenosine diphosphate ribose (cADPR) are

Correspondence: Youxing.Jiang@utsouthwestern.edu.

the three major intracellular Ca^{2+} mobilizing messengers[2]. Among them, NAADP is an endogenous metabolite of β-NADP and is regarded as the most potent Ca^{2+}-releasing second messenger known to date[6,7]. While IP3 and cADPR trigger the Ca^{2+} release from ER, NAADP specifically induces Ca^{2+} release from lysosomes. In animals, lysosomes are acidic organelles containing over 60 different types of hydrolases serving as the center for recycling and degradation of biological materials such as proteins and lipids. Furthermore, lysosomes participate in multiple key cellular activities including autophagy, endocytosis, exocytosis, nutrient sensing[8-12]. Dysfunction of lysosomes could cause numerous diseases, such as type IV mucolipidosis (ML-IV), Parkinson's, Alzheimer's, and Huntington's diseases[12-14]. In fungal and plant cells, vacuoles are the counterparts of lysosomes and serve as the main Ca^{2+} stores[15].

Ca^{2+} homeostasis plays an important role in maintaining the normal function of lysosomes. The luminal Ca^{2+} concentration of a lysosome is approximately 0.5 mM, about five thousand-fold higher than that in the cytosol[16,17]. The lysosomal Ca^{2+} uptake and release are mediated by multiple lysosomal membrane-localized channels and transporters. Two-pore channels (TPCs) and transient receptor potential mucolipin channels (TRPMLs) are the two major lysosome-specific cation channel families that are suggested to be important for lysosomal Ca^{2+} release[18,19]. In addition, multiple plasma membrane channels have also been observed in lysosomal membranes and may conduct Ca^{2+} under certain conditions[3]. These include the purinergic receptor X4 (P2X4)[20,21], the transient receptor potential cation channel subfamily M member 2 (TRPM2)[22], the transient receptor potential ankyrin 1 (TRPA1)[23], and the P/Q-type voltage-gated Ca^{2+} channel (Cav2.1)[24]. In this review, we will primarily focus on the structures and functions of TPCs and TRPMLs, including the plant TPC1 from *Arabidopsis thaliana* (AtTPC1)[25,26], mammalian TPCs from *Mus musculus* and *Homo sapiens* (MmTPC1 and HsTPC2)[27,28], and mammalian TRPML1[29,30].

2. Two-pore channels (TPCs)

TPCs belong to the voltage-gated ion channel superfamily[31] and are ubiquitously expressed in organelles of animals and plants[32,33]. The plant TPC channel (TPC1) is localized to the vacuolar membrane[33,34]. The Mammalian TPC family consists of three isoforms, TPC1, TPC2, and TPC3. TPC1 and 2 are localized to the endolysosomal membrane. They are widely expressed and have been extensively studied[18,35-42]. TPC3 is only present in some mammals and is not expressed in humans. TPC3 has been localized to the lysosomal membrane in chicken and rabbits but the plasma membrane in zebrafish and its functions are not well defined[18,39,43]. TPCs function as a homodimer with each subunit containing 12 transmembrane (TM) segments that can be divided into two homologous copies of the *Shaker-like* 6-TM domain. Thus, TPCs are believed to be evolutionary intermediates between tetrameric voltage-gated K^+ channels and the four-domain single subunit voltage-gated Na^+/Ca^{2+} channels[44]. Plant TPC1 is responsible for generating the slow vacuolar (SV) current observed long before its molecular identification, therefore, plant TPC1 is also called SV channel[33,34,45]. Plant TPC1 is involved in various cellular processes, such as germination and stomatal opening[46], jasmonate biosynthesis[47,48], and long-distance Ca^{2+} wave propagation induced by high salt concentrations[49]. Mammalian TPC1 and TPC2 play critical roles in regulating the physiological functions of lysosomes[12,50,51]. The functions

of mammalian TPCs are implicated in various physiological processes including nutrient sensing[38], autophagy[52,53], lipid metabolism[54], pigmentation[55-57], blood vessel formation[58], and acrosome reaction in sperm[59]. A recent study also indicated that TPCs play an important role in controlling Ebola virus trafficking in host cell[60]. Surprisingly, no TPC mutation has yet been identified to be directly associated with severe human disease[12].

3. Structure and function of the plant TPC1 from *Arabidopsis thaliana*

TPC1 from *Arabidopsis thaliana* (AtTPC1) has been used as the model system for plant TPC and its structures in the closed state were first determined by protein crystallography[25,26]. AtTPC1 is a non-selective cation channel, permeable to various monovalent and divalent cations with a slight preference for Ca^{2+} [61]. The channel is voltage-gated and its activation also requires cytosolic Ca^{2+}. The luminal Ca^{2+}, on the other hand, can inhibit the channel by modulating its voltage gating[62,63]. Each AtTPC1 subunit contains two 6-TM domains (6-TM I and 6-TM II) that are linked by a cytosolic EF-hand domain (Fig. 1A). Two subunits assemble into a rectangle-shaped functional channel equivalent to a tetrameric voltage-gated channel (Fig. 1B). The S1-S4 segment of each 6-TM domain forms the voltage-sensing domain (VSD) at the peripheral of the channel whereas the S5-S6 segment forms the pore domain at the center with S6 lining the ion conduction pathway. Like most classical voltage-gated tetrameric cation channels, the TM region of AtTPC1 is domain swapped with the S1-S4 VSD of one 6-TM interacting with the S5-S6 pore domain of the other 6-TM. The cytosolic EF-hand domain contains two tandem EF-hand motifs and is positioned below the VSD1 from 6-TM I [25,26].

4. Ion conduction pore

Each pore domain (PD 1 and PD 2) contains the outer (S5) and inner (S6) helices and the two pore helices (P1, P2) between them, which is distinct from K^+ channels but similar to Na^+ and Ca^{2+} channels[64-66]. In the closed pore of AtTPC1, the four pore-lining S6s (two IS6s and two IIS6s) form a bundle crossing at the cytosolic side with multiple narrow constriction points, preventing the passage of hydrated cations (Fig. 1C). Those constriction-forming residues include L301s and Y305s from IS6 with the narrowest diagonal distance (atom-to-atom) of about 5.3 Å, and V668s, L672s, and F676s from IIS6 with the narrowest diagonal distance of about 4.2 Å. Different from the K^+ channel whose filter forms a long narrow ion pathway with four well-defined ion binding sites for dehydrated K^+, AtTPC1 has a much shorter and wider selectivity filter formed by residues $_{263}$TTS$_{265}$ in filter 1 and $_{629}$MGN$_{631}$ in filter 2, allowing ions to cross the filter in a hydrated or partially hydrated state[25,26].

5. Voltage-sensing domain

The two VSDs (VSD1 and VSD2) in each AtTPC1 subunit adopt different structures. A few key features important for voltage-dependent gating in canonical voltage-gated channels are present in VSD2 but absent in VSD1 of AtTPC1. These include the presence of multiple gating charge arginines in S4 at every third position separated by two hydrophobic residues between them ($_{537}$**R**ML**R**LI**R**$_{543}$ in the VSD2 of AtTPC1)[25,26,67], the formation

of a 310-helix in part of S4[65,68,69], and the charge transfer center formed of conserved acidic and aromatic residues in S2 and a conserved acidic residue in S3 (Y475 and E478 in S2 and D500 in S3 of AtTPC1) (Fig. 1D) [60,70]. Therefore, only VSD2 contributes to the voltage-dependent gating of AtTPC1[26,28]. Because luminal Ca^{2+} or Ba^{2+} can inhibit the channel activity by stabilizing the voltage sensor in the resting state and Ba^{2+} was present in the crystallization conditions, the VSD2 in the AtTPC1 structure was captured in a resting state, providing crucial insight into the voltage-gating mechanism. In an activated VSD as observed in most structures of voltage-gated channels at the time, the S4 helix tends to be positioned with the side chain of its last gating charge arginine housed in the charge transfer center. In the resting VSD2 of AtTPC1, on contrary, it is the first gating charge arginine (R537) positioned in the gating charge transfer center and this resting state S4 is stabilized directly by a bound luminal divalent ion as described below[25,26] (Fig. 1D). The structural comparison between the activated and resting VSDs suggests that the S4 helix undergoes up and down translational movement in voltage gating and this movement is likely coupled to the pore-lining S6 helix through the linker helix between S4 and S5 (S4-S5 linker)[25,28].

6. Ca^{2+} activation and inhibition

Cytosolic Ca^{2+} potentiates voltage activation of AtTPC1 by binding to the EF-hand domain which contains two EF-hand motifs (EF-1 and 2). In the AtTPC1 structure, the EF-1 motif adopts a canonical Ca^{2+}-bound EF-hand structure but EF-2 is in a Ca^{2+}-free, apo state[25] (Fig. 1E). Interestingly, only the Ca^{2+}-binding at EF-2 plays the determinant role in Ca^{2+} activation whereas Ca^{2+}-binding at EF-1 is dispensable[25,71]. Thus, the structure of the EF-hand domain likely represents a deactivated state, despite the presence of Ca^{2+} in the EF-1 motif. Another interesting feature of the EF-hand domain is that its E1 helix comes from the C-terminal part of the exceptionally long S6 helix (IS6) of 6-TM I, allowing the Ca^{2+}-induced conformational change in the EF-hand domain to be directly coupled to the pore-lining IS6 upon Ca^{2+} activation.

Luminal Ca^{2+} inhibits AtTPC1 by stabilizing the VSD2 in the resting state, thereby shifting the voltage dependence towards positive membrane potentials. Chelated by D454 from IIS1, E528 from IIS4, and D240 from IS5 of the neighboring subunit, the luminal Ca^{2+} tethers the mobile voltage sensing IIS4 to the static IIS1 and the pore-forming IS5 of the neighboring subunit, and thereby hinders IIS4 movement in response to voltage change[25] (Fig. 1F). Consistent with structural observation, one of the key Ca^{2+} coordinating residues, D454, was previously identified to be important for luminal Ca^{2+} binding from a gain-of-function mutant *fou2*[47,48,63].

7. Recent update on AtTPC1 structures

Cryo-EM structures of AtTPC1 in a closed conformation with deactivated EF-hand domain and resting VSD2 and in a partially open conformation with Ca^{2+}-bound EF-hand domain and activated VSD2 were determined recently, revealing the structural basis of voltage gating and cytosolic Ca^{2+} activation of AtTPC1[72] (Fig. 1G-I). In the Ca^{2+}-activated EF-hand domain, its conformational change upon Ca^{2+} binding is directly coupled to the pair of pore-lining IS6 helices, resulting in a wider distance between IS6s at the bundle crossing.

In addition to EF-1 and EF-2 sites, a third Ca^{2+} site important for the Ca^{2+} activation of the channel was also identified in the structure of the Ca^{2+}-bound EF-hand domain. Ca^{2+} at this site is chelated by the side chains of D39 and D43 and several backbone carbonyls at the C-terminal end of the H1 helix (Fig. 1H).

In the activated VSD2 structure, it is the third gating charge arginine (R543) positioned in the gating charge transfer center, confirming the previous suggestion that the IIS4 helix undergoes simple upward translational movement upon voltage activation (Fig. 1I). Intriguingly, in addition to the local IIS4 translation, the entire VSD2 also undergoes a lateral rotation movement around the central pore upon voltage activation. This lateral rotation movement of VSD2 also induces a global rotation of the EF-hand domain which in turn changes the accessibility of the two Ca^{2+} activation sites (EF-2 and the third newly identified Ca^{2+} site). In other words, the voltage activation of VSD2 appears to be a prerequisite for the Ca^{2+} activation at the EF-hand domain.

8. Structures and functions of Mammalian TPCs

Animal TPCs (TPC1 and TPC2) were initially suggested to mediate NAADP-dependent Ca^{2+} release from lysosomes[18,35,36]. However, several recent electrophysiological recordings demonstrate that animal TPCs are Na^{+}-selective channels that can be activated by lysosome-specific phosphatidylinositol 3,5-bisphosphate ($PI(3,5)P_2$) rather than NAADP[37,38]. Debate still lingers on whether TPC1 and TPC2 are directly responsible for NAADP-induced lysosomal Ca^{2+} release. Several recent studies have identified small soluble NAADP-binding proteins that may directly mediate the NAADP-evoked, TPC-dependent Ca^{2+} signaling[73-75]. The activation of TPC1 but not TPC2 is voltage-dependent. TPC3 is also voltage-gated and its voltage gating can be modulated by phosphoinositides such as $PI(3,4)P_2$ and $PI(3,5)P_2$, but not $PI(4,5)P_2$[76]. Different from TPC1, TPC3 is only activated at extreme membrane depolarization and is probably responsible for generating or maintaining ultra-long action potentials[39,77,78]. The structure of TPC3 from zebrafish has also been determined recently[78]. As TPC3 is not present in humans and has been less studied, it will not be further discussed in this review. The following discussion about mammalian TPCs will be focused on the structures of mouse TPC1 (MmTPC1) and human TPC2 (HsTPC2).

Despite low sequence identity between them, mammalian TPCs share a similar overall structure to the plant TPC1[25-28] (Fig. 2A&B). Similar to AtTPC1, the two homologous 6-TM domains of mammalian TPCs are also connected by an EF-hand domain (Fig. 2A-B). However, the EF-hand domain lacks the essential Ca^{2+} chelating acidic residues and the mammalian TPC channels are not Ca^{2+} activated. One unique feature of mammalian TPC1 is that its C-terminal region adopts a horseshoe-shaped structure with four α-helices and two β-strands and wraps tightly around the EF-hand domain (Fig. 2C). It is unclear whether this unique structure feature at the C-terminus plays any functional role[28].

9. Ion conduction pore

Similar to plant TPC1, each pore domain of the mammalian TPCs consists of S5, S6, and two pore helices. In a functional channel dimer, the ion conduction pore consists of two pairs of the pore domains, the IS5-IS6 pair from 6-TM I and the IIS5-IIS6 pair from 6-TM II. The structures of mammalian TPCs were determined in both open and closed conformations, allowing us to visualize the pore opening mechanics[27,28] (Fig. 2D). In the closed structure, the four pore-lining S6 helices form a bundle-crossing at the cytosolic side with narrow hydrophobic constrictions (L317 and F321 in IS6 and V684 and L688 in IIS6) that form the intracellular gate and prevent the passage of hydrated cations. In the open structure, the S6 helices undergo outward movement along with rotational motion, resulting in a much wider opening at the intracellular gate (Fig. 2E). This pore opening is driven by $PI(3,5)P_2$-binding at 6-TM I and the ensued conformational change at the pair of IS6 helices, as will be discussed later[27,28].

Mammalian TPCs have virtually identical sequences and similar structures at the selectivity filter[27,28]. One key difference between mammalian TPCs and plant TPC1 that differentiates their selectivity property lies in the filter (filter 2) from the 2nd 6-TM domain. As in the example of MmTPC1, its filter 2 has a sequence of $_{647}$VNN$_{649}$, whereas the equivalent filter 2 in AtTPC1 is $_{629}$MGN$_{631}$. The side chain of N648 generates a much narrower constriction at the center of the MmTPC1 filter[28] (Fig. 2D). The equivalent residue in plant TPC1 is a glycine (G630 in AtTPC1), yielding a wider ion pathway in the filter (Fig. 1C)[28]. The formation of the narrow point along the filter pathway by a conserved asparagine renders the MmTPC1, as well as other mammalian TPCs, highly Na^+ selective, and its mutation, can result in a complete loss of Na^+ selectivity[27,28]. Conversely, replacing G630 with Asn in AtTPC1 can convert the channel to be more Na^+ selective[61].

10. Voltage-sensing domain

Like AtTPC1, MmTPC1 is voltage-gated with its VSD2 contributing to the voltage activation of the channel[28]. Interestingly, the VSD2 of MmTPC1 adopts an activated conformation in both the apo closed and $PI(3,5)P_2$-bound open structures (Fig. 2F), suggesting that the voltage sensor of MmTPC1 can be activated without opening the channel and $PI(3,5)P_2$ binding is the driving force for channel activation[28]. Although not directly coupled to the pore opening, VSD2 activation appears to be required before $PI(3,5)P_2$-driven channel opening can occur[28]. The VSD2 of MmTPC1 contains only two gating charge arginines with a sequence of $_{540}$**R**PL**Q**LL**R**$_{546}$ at its gating charge region where the middle Arg present in AtTPC1 becomes a Gln in MmTPC1[25,28] (Fig. 1D and Fig. 2F). In the structure of the activated MmTPC1 VSD2, it is the last Arg (R546) positioned in the gating charge transfer center. Interestingly, replacing the first arginine (R540) with Gln or Ile yields a mutant channel analogous to TPC2 which is no longer voltage-gated and can be activated by $PI(3,5)P_2$ alone[39]. This R540 mutation likely stabilizes the VSD2 in an activated state. Replacing the last Arg (R546) with Gln, on the other hand, yields a channel that can barely be activated by voltage even with the presence of high concentration $PI(3,5)P_2$, as if the voltage sensor of the mutant is trapped in the resting state[28]. Structural comparison between

the activated VSD2 of MmTPC1 and the resting VSD2 of AtTPC1 reveals about 2-helical turn upward slide of the IIS4 upon voltage activation in TPC1[25,28].

Interestingly, the structure of VSD2 from HsTPC2 resembles that of MmTPC1 but the channel activation is not voltage dependent[27,28]. The gating charge region of HsTPC2 VSD2 has a sequence of $_{551}$IVF**R**FL**R**$_{557}$ with its first arginine placed in the middle position instead of the first position observed in MmTPC1 (Fig. 1D and Fig. 2G). The S4 of HsTPC2 VSD2 is positioned with its middle arginine (R554) occupying the gating charge transfer center[27]. In most mammalian TPC2, there is an Ile instead of Arg at the beginning of the VSD2 gating charge region. When the first Ile (I551) is replaced with Arg in HsTPC2, the mutant channel becomes voltage-gated and requires both PI(3,5)P_2 and voltage for its activation[27]. Thus, the presence or absence of the first Arg at the gating charge region appears to determine the voltage dependence of mammalian TPC channels.

11. PI(3,5)P_2 binding

In mammalian TPCs, PI(3,5)P_2 binds within the first 6-TM domain at the junction formed by IS3, IS4, and the IS4-S5 linker, and its inositol 1,3,5-trisphosphate (Ins(1,3,5)P3) head group involves in most of the ligand-protein interactions[27,28]. As in the example of PI(3,5)P_2-bound MmTPC1 structure, the protein residues that participate in ligand interactions are predominantly basic (Fig. 2H). Some basic residues, including R220, R221, and R224 in the IS4-S5 linker and K331 on IS6, directly interact with the phosphate group on the C3 position of the lipid head group and play critical roles in PI(3,5)P_2 binding and channel activation[28]. The PI(3,5)P_2 binding site in HsTPC2 is similar to that in MmTPC1[27]. One notable difference between them is that most of the basic residues involved in ligand interactions, particularly those in the IS4-S5 linker, are predominantly lysines (K203, K204, and K207) in HsTPC2 rather than arginines (Fig. 2I). Mammalian TPCs have high ligand specificity and PI(4,5)P_2 cannot activate the channel. Based on the PI(3,5)P2-bound MmTPC1 structure, this can be explained by missing the C3-phosphate in PI(4,5)P2 lipid that is central for ligand-protein interactions, and the proximity of protein residues (Asn85 and Lys87 in MmTPC1) to the C4 hydroxyl group of the ligand, which occludes the space for the C4-phosphate and thereby sterically prevents PI(4,5)P_2 binding [27,28]. PI(3,5)P_2 binding activates the MmTPC1 channel by pulling IS6 towards the ligand-binding pocket through the interactions between K331 in IS6 and the phosphate groups of the ligand. This movement propagates to the other part of the IS6 helix, resulting in the outward dilation and rotation movements of those constriction-forming residues. To accommodate the conformational change at IS6 and open the pore, the other constriction-forming residues on IIS6 must undergo similar dilation and rotation movements[28]. Based on the structural comparison between the open and closed MmTPC1, it was proposed that this concurrent movement of IIS6 in response to the PI(3,5)P_2-induced conformational change at IS6 can only occur when IIS4 of VSD2 is in the activated, up state[28].

12. Transient Receptor Potential Mucolipin (TRPML)

TRPMLs are Ca^{2+}-permeable non-selective cation channels that belong to the large family of TRP ion channels[79]. TRPML family consists of three isoforms, TRPML1, TRPML2,

and TRPML3, which share high homology in amino acid sequence but are expressed in different tissues[80,81]. TRPML1 is ubiquitously expressed in mammalian cells and is primarily localized to the lysosomal membrane [82]. In contrast, the tissue expression of TRPML2 and TRPML3 is more restricted. TRPML2 is expressed in the thymus, spleen, and kidney [83,84], and TRPML3 is expressed in the kidney, lung, and organs of the endocrine system[85]. TRPMLs involve in multiple important cellular activities including lysosome trafficking, lipid accumulation, signaling transduction, and autophagy[8-11,86]. Mutations in TRPML1 can directly cause the lysosomal storage disorder mucolipidosis type IV (MLIV), a neurodegenerative disease characterized by abnormal neurodevelopment, retinal degeneration, and iron deficiency anaemia[13,14,87,88]. Gain-of-function mutations in mouse TRPML3 attribute to the varitint-waddler (*Va*) phenotype with symptoms including deafness, pigmentation defects, and circling behavior[19,89].

13. The overall structure of TRPML

Multiple TRPML structures have been determined in various states[29,30,90-95]. TRPMLs are 6-TM tetrameric cation channels and are comprised of two structural components: the membrane-embedded S1-S6 transmembrane domain (TMD) and the canopy-like luminal linker domain atop the TMD[29,30,90] (Fig. 3A&B). Like most canonical 6-TM tetrameric channels, the TMD of TRPML is divided into two parts, the S1-S4 VSD and the S5-S6 pore domain, connected by the S4-S5 linker helix[30]. The VSD resembles other TRP channels by having four straight helices tightly packed against each other but differs from the canonical VSD of voltage-gated channels by lacking the canonical voltage sensing arginines. The ion conduction pore is formed by S5, S6, and two pore helices (P1 and P2). Different from TRPV1 whose filter can undergo a remarkable conformational change upon ligand activation[77,78], the selectivity filter of TRPML is tightly packed with P1 and P2 helices and is unlikely to undergo major conformation change during gating[29,30,90]. The luminal linker domain contains a sequence of about 200 amino acids between S1 and S2 (Fig. 3A&B). Structurally, each luminal linker domain is comprised of two long helices and seven strands; four linker domains form a square-shaped canopy with a central hole above the channel pore in a channel tetramer, which is a characteristic feature of group II TRP channels including TRPML and TRPP[79,96] (Fig. 3A-3C). In the polycystic kidney disease channel PKD2, a member of the TRPP family, this linker domain is referred to as the polycystin or top domain[96]. TRPML possesses two unique cytosolic extensions: an N-terminal pre-S1 cytosolic domain containing two short helixes (H1 and H2) enriched in basic residues and a helix–turn–helix (H3–turn–H4) between S2 and S3. Another distinct feature of TRPMLs is the lack of TRP domain, a short peptide sequence around 25 amino acids immediately after S6 that is commonly seen in other TRP family channels, including the TRPC, V, M subfamilies[97,98].

14. The modulation of TRPMLs by natural and synthetic ligands

TRPMLs can be activated or inhibited by various ligands, including natural and synthetic molecules. Endogenously, TRPMLs can be activated by lysosome-specific $PI(3,5)P_2$[99], but inhibited by $PI(4,5)P_2$ enriched in plasma membrane [100]. In addition, sphingomyelins have been shown to inhibit the activity of TRPML1, and such inhibition is reversed by

treating with sphingomyelinase[9]. Multiple synthetic agonists and antagonists have been identified through drug screenings and development[9,101-104]. ML-SA1 is the most well-characterized agonist that can robustly activate TRPML by itself as well as synergistically with $PI(3,5)P_2$[9,102]. In addition to agonists, several antagonists with different chemical structures were identified, such as ML-SI1, 2, and 3. Some of these antagonists are capable of inhibiting both ML-SA1 and $PI(3,5)P_2$-elicited TRPML currents[103]. Furthermore, two recent studies suggested that rapamycin and reactive oxygen species can both directly and specifically activate TRPML in an mTOR-independent manner[105,106].

The structures of TRPML1 in complex with $PI(3,5)P_2$ or $PI(4,5)P_2$ reveal that both lipids bind to the same N-terminal poly-basic region formed by cytosol-extruding H1 and H2, which is distal from the pore region[94] (Fig. 3D). As the structure of $PI(3,5)P_2$-bound TRPML1 (in the absence of other agonists) remains in the closed conformation likely because of the low open probability of channel upon $PI(3,5)P_2$ activation, it is unclear how $PI(3,5)P_2$ induces the conformational changes that open the channel[30,94]. It was proposed that the binding of $PI(3,5)P_2$ and the ensued interaction between its C3 phosphate and Y355 in S3 promote the formation of a π-cation interaction between Y355 and R403 in S4, which in turn facilitates the pore opening[94]. However, as those PIP_2-bound structures are of low resolution, the protein-ligand and protein-protein interactions at the lipid-binding site could not be accurately defined.

As a potent agonist, the ML-SA1-bound structure captured the TRPML1 channel in an open conformation[29]. ML-SA1 resides in a hydrophobic pocket formed by several aromatic and hydrophobic residues from P1, S5, S6, and S6 of the neighboring subunit (Fig. 3E). The binding of ML-SA1 causes the pore-forming S5 and S6 to shift slightly away from the pore center, resulting in the opening of the lower gate. To accommodate the ML-SA1 binding and its induced lower gate-opening S6 movement, the filter region including the two pore helices and the selectivity filter also moves slightly away from the center, resulting in a subtle enlargement of the filter pathway [29,94].

Recently, the antagonist ML-SI3-bound human TRPML1 structure was reported[92] (Fig. 3F). The structure is in a closed conformation and is virtually identical to the apo structure. ML-SI3 binds at the same hydrophobic cavity as ML-SA1 does, explaining ML-SI3's competitive inhibition of ML-SA1 activation of TRPML1. However, the two chemicals engage in a different set of protein-ligand interactions, rendering one (ML-SA1) to be agonist whereas the other (ML-SI3) to be antagonist.

15. The modulation of TRPMLs by pH and Ca^{2+}

The TRPML activity is also regulated by pH and Ca^{2+} concentration in both lysosomal lumen and cytoplasm sides[80,107-109]. Increasing luminal Ca^{2+} concentration inhibits the channel conductance in a dose-dependent manner. The luminal Ca^{2+}-inhibition is pH-dependent as lowering the luminal pH can rescue the inhibition[107]. Several aspartate residues, including D111, D114, and D115 in both human and mouse TRPML1, are positioned in proximity to the central ion pathway of the luminal linker domain and have been shown to contribute to the pH-dependent luminal Ca^{2+}-inhibition of TRPML1[95]. With

an acidic luminal environment in the lysosome, the protonation of these acidic residues likely mitigates the Ca^{2+} inhibition of TRPML1 under physiological conditions. Contrary to the promotion of ion conduction by reducing Ca^{2+} inhibition in TRPML1, it has been shown that lower extracytosolic (luminal or extracellular) pH inhibits Na^+ or Ca^{2+} conduction in TRPML3 and this pH-dependent regulation is mediated by a string of histidines in the luminal linker domain[110]. In addition, the linker domain has also been shown to be responsible for the inhibition of TRPML2 and TRPML3 by extracytosolic Na^+ [111,112]. It was suggested that in normal cells, the lysosomal Na^+ concentration is high enough to keep TRPML3 inactive. However, the channel can become active when the lysosome is damaged or the lysosomal Na^+ and H^+ gradient break down [91,110,111]. A study suggests that pathogen-induced pH neutralization of lysosome triggers Ca^{2+} release by activating TRPML3, which in turn facilitates lysosome exocytosis and expulsion of the phagocyted bacteria pathogens[113].

Acknowledgments

Youxing Jiang is supported in part by the Howard Hughes Medical Institute and by grants from the National Institute of Health (R35GM140892), and the Welch Foundation (Grant I-1578). Ninghai Gan is an HHMI fellow of the Jane Coffin Childs Memorial Fund.

References

1. Berridge MJ, Lipp P & Bootman MD The versatility and universality of calcium signalling. Nature reviews. Molecular cell biology 1, 11–21, doi:10.1038/35036035 (2000). [PubMed: 11413485]
2. Clapham DE Calcium Signaling. Cell 131, 1047–1058, doi:10.1016/j.cell.2007.11.028 (2007). [PubMed: 18083096]
3. Yang J, Zhao Z, Gu M, Feng X & Xu H Release and uptake mechanisms of vesicular Ca(2+) stores. Protein Cell 10, 8–19, doi:10.1007/s13238-018-0523-x (2019). [PubMed: 29549599]
4. Luan S & Wang C Calcium Signaling Mechanisms Across Kingdoms. Annu Rev Cell Dev Biol 37, 311–340, doi:10.1146/annurev-cellbio-120219-035210 (2021). [PubMed: 34375534]
5. Pozzan T, Rizzuto R, Volpe P & Meldolesi J Molecular and cellular physiology of intracellular calcium stores. Physiol Rev 74, 595–636, doi:10.1152/physrev.1994.74.3.595 (1994). [PubMed: 8036248]
6. Lee HC & Aarhus R A derivative of NADP mobilizes calcium stores insensitive to inositol trisphosphate and cyclic ADP-ribose. The Journal of biological chemistry 270, 2152–2157, doi:10.1074/jbc.270.5.2152 (1995). [PubMed: 7836444]
7. Galione A NAADP Receptors. Cold Spring Harbor perspectives in biology 11, doi:10.1101/cshperspect.a035071 (2019).
8. Venkatachalam K, Wong CO & Zhu MX The role of TRPMLs in endolysosomal trafficking and function. Cell Calcium 58, 48–56, doi:10.1016/j.ceca.2014.10.008 (2015). [PubMed: 25465891]
9. Shen D et al. Lipid storage disorders block lysosomal trafficking by inhibiting a TRP channel and lysosomal calcium release. Nat Commun 3, 731, doi:10.1038/ncomms1735 (2012). [PubMed: 22415822]
10. Kilpatrick BS, Yates E, Grimm C, Schapira AH & Patel S Endo-lysosomal TRP mucolipin-1 channels trigger global ER Ca2+ release and Ca2+ influx. J Cell Sci 129, 3859–3867, doi:10.1242/jcs.190322 (2016). [PubMed: 27577094]
11. Scotto Rosato A et al. TRPML1 links lysosomal calcium to autophagosome biogenesis through the activation of the CaMKKβ/VPS34 pathway. Nature Communications 10, 5630, doi:10.1038/s41467-019-13572-w (2019).
12. Xu H & Ren D Lysosomal physiology. Annu Rev Physiol 77, 57–80, doi:10.1146/annurev-physiol-021014-071649 (2015). [PubMed: 25668017]

13. Bargal R et al. Identification of the gene causing mucolipidosis type IV. Nat Genet 26, 118–123, doi:10.1038/79095 (2000). [PubMed: 10973263]
14. Sun M et al. Mucolipidosis type IV is caused by mutations in a gene encoding a novel transient receptor potential channel. Hum Mol Genet 9, 2471–2478, doi:10.1093/hmg/9.17.2471 (2000). [PubMed: 11030752]
15. Marty F Plant Vacuoles. The Plant Cell 11, 587–599, doi:10.1105/tpc.11.4.587 (1999). [PubMed: 10213780]
16. Christensen KA, Myers JT & Swanson JA pH-dependent regulation of lysosomal calcium in macrophages. J Cell Sci 115, 599–607 (2002). [PubMed: 11861766]
17. Srinivas SP, Ong A, Goon L, Goon L & Bonanno JA Lysosomal Ca(2+) stores in bovine corneal endothelium. Invest Ophthalmol Vis Sci 43, 2341–2350 (2002). [PubMed: 12091436]
18. Calcraft PJ et al. NAADP mobilizes calcium from acidic organelles through two-pore channels. Nature 459, 596–600, doi:10.1038/nature08030 (2009). [PubMed: 19387438]
19. Xu H, Delling M, Li L, Dong X & Clapham DE Activating mutation in a mucolipin transient receptor potential channel leads to melanocyte loss in varitint-waddler mice. Proc Natl Acad Sci U S A 104, 18321–18326, doi:10.1073/pnas.0709096104 (2007). [PubMed: 17989217]
20. Qureshi OS, Paramasivam A, Yu JC & Murrell-Lagnado RD Regulation of P2X4 receptors by lysosomal targeting, glycan protection and exocytosis. J Cell Sci 120, 3838–3849, doi:10.1242/jcs.010348 (2007). [PubMed: 17940064]
21. Huang P et al. P2X4 forms functional ATP-activated cation channels on lysosomal membranes regulated by luminal pH. J Biol Chem 289, 17658–17667, doi:10.1074/jbc.M114.552158 (2014). [PubMed: 24817123]
22. Lange I et al. TRPM2 functions as a lysosomal Ca2+-release channel in beta cells. Sci Signal 2, ra23, doi:10.1126/scisignal.2000278 (2009). [PubMed: 19454650]
23. Shang S et al. Intracellular TRPA1 mediates Ca2+ release from lysosomes in dorsal root ganglion neurons. J Cell Biol 215, 369–381, doi:10.1083/jcb.201603081 (2016). [PubMed: 27799370]
24. Tian X et al. A voltage-gated calcium channel regulates lysosomal fusion with endosomes and autophagosomes and is required for neuronal homeostasis. PLoS Biol 13, e1002103, doi:10.1371/journal.pbio.1002103 (2015). [PubMed: 25811491]
25. Guo J et al. Structure of the voltage-gated two-pore channel TPC1 from Arabidopsis thaliana. Nature 531, 196–201, doi:10.1038/nature16446 (2016). [PubMed: 26689363]
26. Kintzer AF & Stroud RM Structure, inhibition and regulation of two-pore channel TPC1 from Arabidopsis thaliana. Nature 531, 258–262, doi:10.1038/nature17194 (2016). [PubMed: 26961658]
27. She J et al. Structural mechanisms of phospholipid activation of the human TPC2 channel. Elife 8, doi:10.7554/eLife.45222 (2019).
28. She J et al. Structural insights into the voltage and phospholipid activation of the mammalian TPC1 channel. Nature 556, 130–134, doi:10.1038/nature26139 (2018). [PubMed: 29562233]
29. Schmiege P, Fine M, Blobel G & Li X Human TRPML1 channel structures in open and closed conformations. Nature 550, 366–370, doi:10.1038/nature24036 (2017). [PubMed: 29019983]
30. Chen Q et al. Structure of mammalian endolysosomal TRPML1 channel in nanodiscs. Nature 550, 415–418, doi:10.1038/nature24035 (2017). [PubMed: 29019981]
31. Yu FH & Catterall WA The VGL-chanome: a protein superfamily specialized for electrical signaling and ionic homeostasis. Sci STKE 2004, re15, doi:10.1126/stke.2532004re15 (2004). [PubMed: 15467096]
32. Ishibashi K, Suzuki M & Imai M Molecular cloning of a novel form (two-repeat) protein related to voltage-gated sodium and calcium channels. Biochemical and biophysical research communications 270, 370–376, doi:10.1006/bbrc.2000.2435 (2000). [PubMed: 10753632]
33. Furuichi T, Cunningham KW & Muto S A putative two pore channel AtTPC1 mediates Ca(2+) flux in Arabidopsis leaf cells. Plant & cell physiology 42, 900–905 (2001). [PubMed: 11577183]
34. Hedrich R & Neher E Cytoplasmic calcium regulates voltage-dependent ion channels in plant vacuoles. Nature 329, 833–836, doi:10.1038/329833a0 (1987).

35. Brailoiu E et al. Essential requirement for two-pore channel 1 in NAADP-mediated calcium signaling. J Cell Biol 186, 201–209, doi:10.1083/jcb.200904073 (2009). [PubMed: 19620632]
36. Zong X et al. The two-pore channel TPCN2 mediates NAADP-dependent Ca(2+)-release from lysosomal stores. Pflugers Archiv : European journal of physiology 458, 891–899, doi:10.1007/s00424-009-0690-y (2009). [PubMed: 19557428]
37. Wang X et al. TPC proteins are phosphoinositide- activated sodium-selective ion channels in endosomes and lysosomes. Cell 151, 372–383, doi:10.1016/j.cell.2012.08.036 (2012). [PubMed: 23063126]
38. Cang C et al. mTOR regulates lysosomal ATP-sensitive two-pore Na(+) channels to adapt to metabolic state. Cell 152, 778–790, doi:10.1016/j.cell.2013.01.023 (2013). [PubMed: 23394946]
39. Cang C, Bekele B & Ren D The voltage-gated sodium channel TPC1 confers endolysosomal excitability. Nature chemical biology 10, 463–469, doi:10.1038/nchembio.1522 (2014). [PubMed: 24776928]
40. Jha A, Ahuja M, Patel S, Brailoiu E & Muallem S Convergent regulation of the lysosomal two-pore channel-2 by Mg(2)(+), NAADP, PI(3,5)P(2) and multiple protein kinases. EMBO J 33, 501–511, doi:10.1002/embj.201387035 (2014). [PubMed: 24502975]
41. Pitt SJ, Lam AKM, Rietdorf K, Galione A & Sitsapesan R Reconstituted Human TPC1 Is a Proton-Permeable Ion Channel and Is Activated by NAADP or Ca2+. Science Signaling 7, doi:ARTN ra46 10.1126/scisignal.2004854 (2014). [PubMed: 24847115]
42. Ruas M et al. Expression of Ca(2)(+)-permeable two-pore channels rescues NAADP signalling in TPC-deficient cells. EMBO J 34, 1743–1758, doi:10.15252/embj.201490009 (2015). [PubMed: 25872774]
43. Ogunbayo OA et al. Organelle-specific subunit interactions of the vertebrate two-pore channel family. J Biol Chem 290, 1086–1095, doi:10.1074/jbc.M114.610493 (2015). [PubMed: 25451935]
44. Rahman T et al. Two-pore channels provide insight into the evolution of voltage-gated Ca2+ and Na+ channels. Science signaling 7, ra109, doi:10.1126/scisignal.2005450 (2014). [PubMed: 25406377]
45. Hedrich R & Marten I TPC1-SV channels gain shape. Molecular plant 4, 428–441, doi:10.1093/mp/ssr017 (2011). [PubMed: 21459829]
46. Peiter E et al. The vacuolar Ca2+-activated channel TPC1 regulates germination and stomatal movement. Nature 434, 404–408, doi:10.1038/nature03381 (2005). [PubMed: 15772667]
47. Bonaventure G et al. A gain-of-function allele of TPC1 activates oxylipin biogenesis after leaf wounding in Arabidopsis. Plant Journal 49, 889–898, doi:10.1111/j.1365-313X.2006.03002.x (2007).
48. Bonaventure G, Gfeller A, Rodriguez VM, Armand F & Farmer EE The fou2 gain-of-function allele and the wild-type allele of Two pore channel 1 contribute to different extents or by different mechanisms to defense gene expression in Arabidopsis. Plant and Cell Physiology 48, 1775–1789, doi:10.1093/pcp/pcm151 (2007). [PubMed: 17981874]
49. Choi WG, Toyota M, Kim SH, Hilleary R & Gilroy S Salt stress-induced Ca2+ waves are associated with rapid, long-distance root-to-shoot signaling in plants. Proceedings of the National Academy of Sciences of the United States of America 111, 6497–6502, doi:10.1073/pnas.1319955111 (2014). [PubMed: 24706854]
50. Patel S Function and dysfunction of two-pore channels. Sci Signal 8, re7, doi:10.1126/scisignal.aab3314 (2015). [PubMed: 26152696]
51. Grimm C, Chen CC, Wahl-Schott C & Biel M Two-Pore Channels: Catalyzers of Endolysosomal Transport and Function. Front Pharmacol 8, 45, doi:10.3389/fphar.2017.00045 (2017). [PubMed: 28223936]
52. Fernandez B et al. Iron overload causes endolysosomal deficits modulated by NAADP-regulated 2-pore channels and RAB7A. Autophagy 12, 1487–1506, doi:10.1080/15548627.2016.1190072 (2016). [PubMed: 27383256]
53. Pereira GJ et al. Nicotinic acid adenine dinucleotide phosphate (NAADP) regulates autophagy in cultured astrocytes. J Biol Chem 286, 27875–27881, doi:10.1074/jbc.C110.216580 (2011). [PubMed: 21610076]

54. Grimm C et al. High susceptibility to fatty liver disease in two-pore channel 2-deficient mice. Nat Commun 5, 4699, doi:10.1038/ncomms5699 (2014). [PubMed: 25144390]
55. Ambrosio AL, Boyle JA, Aradi AE, Christian KA & Di Pietro SM TPC2 controls pigmentation by regulating melanosome pH and size. Proc Natl Acad Sci U S A 113, 5622–5627, doi:10.1073/pnas.1600108113 (2016). [PubMed: 27140606]
56. Bellono NW, Escobar IE & Oancea E A melanosomal two-pore sodium channel regulates pigmentation. Sci Rep 6, 26570, doi:10.1038/srep26570 (2016). [PubMed: 27231233]
57. Sulem P et al. Two newly identified genetic determinants of pigmentation in Europeans. Nature genetics 40, 835–837, doi:10.1038/ng.160 (2008). [PubMed: 18488028]
58. Favia A et al. VEGF-induced neoangiogenesis is mediated by NAADP and two-pore channel-2-dependent Ca2+ signaling. Proc Natl Acad Sci U S A 111, E4706–4715, doi:10.1073/pnas.1406029111 (2014). [PubMed: 25331892]
59. Arndt L et al. NAADP and the two-pore channel protein 1 participate in the acrosome reaction in mammalian spermatozoa. Mol Biol Cell 25, 948–964, doi:10.1091/mbc.E13-09-0523 (2014). [PubMed: 24451262]
60. Sakurai Y et al. Ebola virus. Two-pore channels control Ebola virus host cell entry and are drug targets for disease treatment. Science 347, 995–998, doi:10.1126/science.1258758 (2015). [PubMed: 25722412]
61. Guo J, Zeng W & Jiang Y Tuning the ion selectivity of two-pore channels. Proc Natl Acad Sci U S A 114, 1009–1014, doi:10.1073/pnas.1616191114 (2017). [PubMed: 28096396]
62. Pottosin II, Martínez-Estévez M, Dobrovinskaya OR, Muñiz J & Schönknecht G Mechanism of luminal Ca2+ and Mg2+ action on the vacuolar slowly activating channels. Planta 219, 1057–1070, doi:10.1007/s00425-004-1293-7 (2004). [PubMed: 15605179]
63. Dadacz-Narloch B et al. A novel calcium binding site in the slow vacuolar cation channel TPC1 senses luminal calcium levels. The Plant cell 23, 2696–2707, doi:10.1105/tpc.111.086751 (2011). [PubMed: 21764990]
64. Doyle DA et al. The structure of the potassium channel: molecular basis of K+ conduction and selectivity. Science 280, 69–77 (1998). [PubMed: 9525859]
65. Payandeh J, Scheuer T, Zheng N & Catterall WA The crystal structure of a voltage-gated sodium channel. Nature 475, 353–358, doi:10.1038/nature10238 (2011). [PubMed: 21743477]
66. Wu J et al. Structure of the voltage-gated calcium channel Cav1.1 complex. Science 350, aad2395, doi:10.1126/science.aad2395 (2015). [PubMed: 26680202]
67. Catterall WA Ion Channel Voltage Sensors: Structure, Function, and Pathophysiology. Neuron 67, 915–928, doi:10.1016/j.neuron.2010.08.021 (2010). [PubMed: 20869590]
68. Long SB, Tao X, Campbell EB & MacKinnon R Atomic structure of a voltage-dependent K+ channel in a lipid membrane-like environment. Nature 450, 376–382, doi:10.1038/nature06265 (2007). [PubMed: 18004376]
69. Vieira-Pires RS & Morais-Cabral JH 3(10) helices in channels and other membrane proteins. J Gen Physiol 136, 585–592, doi:10.1085/jgp.201010508 (2010). [PubMed: 21115694]
70. Tao X, Lee A, Limapichat W, Dougherty DA & MacKinnon R A gating charge transfer center in voltage sensors. Science 328, 67–73, doi:10.1126/science.1185954 (2010). [PubMed: 20360102]
71. Schulze C, Sticht H, Meyerhoff P & Dietrich P Differential contribution of EF-hands to the Ca(2)(+)-dependent activation in the plant two-pore channel TPC1. The Plant journal : for cell and molecular biology 68, 424–432, doi:10.1111/j.1365-313X.2011.04697.x (2011). [PubMed: 21736651]
72. Ye F et al. Voltage-gating and cytosolic Ca(2+) activation mechanisms of Arabidopsis two-pore channel AtTPC1. Proc Natl Acad Sci U S A 118, doi:10.1073/pnas.2113946118 (2021).
73. Gunaratne GS et al. Essential requirement for JPT2 in NAADP-evoked Ca(2+) signaling. Sci Signal 14, doi:10.1126/scisignal.abd5605 (2021).
74. Roggenkamp HG et al. HN1L/JPT2: A signaling protein that connects NAADP generation to Ca(2+) microdomain formation. Sci Signal 14, doi:10.1126/scisignal.abd5647 (2021).
75. Zhang J, Guan X, Shah K & Yan J Lsm12 is an NAADP receptor and a two-pore channel regulatory protein required for calcium mobilization from acidic organelles. Nature Communications 12, 4739, doi:10.1038/s41467-021-24735-z (2021).

76. Shimomura T & Kubo Y Phosphoinositides modulate the voltage dependence of two-pore channel 3. J Gen Physiol 151, 986–1006, doi:10.1085/jgp.201812285 (2019). [PubMed: 31182502]
77. Rybalchenko V et al. Membrane potential regulates nicotinic acid adenine dinucleotide phosphate (NAADP) dependence of the pH- and Ca2+-sensitive organellar two-pore channel TPC1. J Biol Chem 287, 20407–20416, doi:10.1074/jbc.M112.359612 (2012). [PubMed: 22500018]
78. Dickinson MS, Myasnikov A, Eriksen J, Poweleit N & Stroud RM Resting state structure of the hyperdepolarization activated two-pore channel 3. Proceedings of the National Academy of Sciences 117, 1988–1993, doi:10.1073/pnas.1915144117 (2020).
79. Nilius B & Owsianik G The transient receptor potential family of ion channels. Genome Biology 12, 218, doi:10.1186/gb-2011-12-3-218 (2011). [PubMed: 21401968]
80. Dong XP et al. The type IV mucolipidosis-associated protein TRPML1 is an endolysosomal iron release channel. Nature 455, 992–996, doi:10.1038/nature07311 (2008). [PubMed: 18794901]
81. Cheng X, Shen D, Samie M & Xu H Mucolipins: Intracellular TRPML1-3 channels. FEBS Lett 584, 2013–2021, doi:10.1016/j.febslet.2009.12.056 (2010). [PubMed: 20074572]
82. Falardeau JL et al. Cloning and characterization of the mouse Mcoln1 gene reveals an alternatively spliced transcript not seen in humans. BMC Genomics 3, 3, doi:10.1186/1471-2164-3-3 (2002). [PubMed: 11897010]
83. Lindvall JM, Blomberg KE, Wennborg A & Smith CI Differential expression and molecular characterisation of Lmo7, Myo1e, Sash1, and Mcoln2 genes in Btk-defective B-cells. Cell Immunol 235, 46–55, doi:10.1016/j.cellimm.2005.07.001 (2005). [PubMed: 16137664]
84. Samie MA et al. The tissue-specific expression of TRPML2 (MCOLN-2) gene is influenced by the presence of TRPML1. Pflugers Arch 459, 79–91, doi:10.1007/s00424-009-0716-5 (2009). [PubMed: 19763610]
85. Grimm C, Barthmes M & Wahl-Schott C TRPML3. Handb Exp Pharmacol 222, 659–674, doi:10.1007/978-3-642-54215-2_26 (2014). [PubMed: 24756725]
86. Lee JH et al. Presenilin 1 Maintains Lysosomal Ca(2+) Homeostasis via TRPML1 by Regulating vATPase-Mediated Lysosome Acidification. Cell Rep 12, 1430–1444, doi:10.1016/j.celrep.2015.07.050 (2015). [PubMed: 26299959]
87. Bassi MT et al. Cloning of the gene encoding a novel integral membrane protein, mucolipidin-and identification of the two major founder mutations causing mucolipidosis type IV. Am J Hum Genet 67, 1110–1120, doi:10.1016/s0002-9297(07)62941-3 (2000). [PubMed: 11013137]
88. Nilius B, Owsianik G, Voets T & Peters JA Transient receptor potential cation channels in disease. Physiol Rev 87, 165–217, doi:10.1152/physrev.00021.2006 (2007). [PubMed: 17237345]
89. Di Palma F et al. Mutations in Mcoln3 associated with deafness and pigmentation defects in varitint-waddler (Va) mice. Proc Natl Acad Sci U S A 99, 14994–14999, doi:10.1073/pnas.222425399 (2002). [PubMed: 12403827]
90. Hirschi M et al. Cryo-electron microscopy structure of the lysosomal calcium-permeable channel TRPML3. Nature 550, 411–414, doi:10.1038/nature24055 (2017). [PubMed: 29019979]
91. Zhou X et al. Cryo-EM structures of the human endolysosomal TRPML3 channel in three distinct states. Nature Structural & Molecular Biology 24, 1146–1154, doi:10.1038/nsmb.3502 (2017).
92. Schmiege P, Fine M & Li X Atomic insights into ML-SI3 mediated human TRPML1 inhibition. Structure, doi:10.1016/j.str.2021.06.003 (2021).
93. Viet KK et al. Structure of the Human TRPML2 Ion Channel Extracytosolic/Lumenal Domain. Structure 27, 1246–1257.e1245, doi:10.1016/j.str.2019.04.016 (2019). [PubMed: 31178222]
94. Fine M, Schmiege P & Li X Structural basis for PtdInsP(2)-mediated human TRPML1 regulation. Nat Commun 9, 4192, doi:10.1038/s41467-018-06493-7 (2018). [PubMed: 30305615]
95. Li M et al. Structural basis of dual Ca(2+)/pH regulation of the endolysosomal TRPML1 channel. Nat Struct Mol Biol 24, 205–213, doi:10.1038/nsmb.3362 (2017). [PubMed: 28112729]
96. Shen PS et al. The Structure of the Polycystic Kidney Disease Channel PKD2 in Lipid Nanodiscs. Cell 167, 763–773.e711, doi:10.1016/j.cell.2016.09.048 (2016). [PubMed: 27768895]
97. Zhu X, Chu PB, Peyton M & Birnbaumer L Molecular cloning of a widely expressed human homologue for the Drosophila trp gene. FEBS Lett 373, 193–198, doi:10.1016/0014-5793(95)01038-g (1995). [PubMed: 7589464]

98. Steinberg X, Lespay-Rebolledo C & Brauchi S A structural view of ligand-dependent activation in thermoTRP channels. Front Physiol 5, 171, doi:10.3389/fphys.2014.00171 (2014). [PubMed: 24847275]

99. Dong XP et al. PI(3,5)P(2) controls membrane trafficking by direct activation of mucolipin Ca(2+) release channels in the endolysosome. Nat Commun 1, 38, doi:10.1038/ncomms1037 (2010). [PubMed: 20802798]

100. Zhang X, Li X & Xu H Phosphoinositide isoforms determine compartment-specific ion channel activity. Proc Natl Acad Sci U S A 109, 11384–11389, doi:10.1073/pnas.1202194109 (2012). [PubMed: 22733759]

101. Wang W et al. Up-regulation of lysosomal TRPML1 channels is essential for lysosomal adaptation to nutrient starvation. Proc Natl Acad Sci U S A 112, E1373–1381, doi:10.1073/pnas.1419669112 (2015). [PubMed: 25733853]

102. Grimm C et al. Small molecule activators of TRPML3. Chem Biol 17, 135–148, doi:10.1016/j.chembiol.2009.12.016 (2010). [PubMed: 20189104]

103. Samie M et al. A TRP channel in the lysosome regulates large particle phagocytosis via focal exocytosis. Dev Cell 26, 511–524, doi:10.1016/j.devcel.2013.08.003 (2013). [PubMed: 23993788]

104. Chen CC et al. A small molecule restores function to TRPML1 mutant isoforms responsible for mucolipidosis type IV. Nat Commun 5, 4681, doi:10.1038/ncomms5681 (2014). [PubMed: 25119295]

105. Zhang X et al. Rapamycin directly activates lysosomal mucolipin TRP channels independent of mTOR. PLoS Biol 17, e3000252, doi:10.1371/journal.pbio.3000252 (2019). [PubMed: 31112550]

106. Zhang X et al. MCOLN1 is a ROS sensor in lysosomes that regulates autophagy. Nature Communications 7, 12109, doi:10.1038/ncomms12109 (2016).

107. Suurväli J, Boudinot P, Kanellopoulos J & Rüütel Boudinot S P2X4: A fast and sensitive purinergic receptor. Biomed J 40, 245–256, doi:10.1016/j.bj.2017.06.010 (2017). [PubMed: 29179879]

108. Xu H, Delling M, Li L, Dong X & Clapham DE Activating mutation in a mucolipin transient receptor potential channel leads to melanocyte loss in varitint–waddler mice. Proceedings of the National Academy of Sciences 104, 18321–18326, doi:10.1073/pnas.0709096104 (2007).

109. Dong XP, Wang X & Xu H TRP channels of intracellular membranes. J Neurochem 113, 313–328, doi:10.1111/j.1471-4159.2010.06626.x (2010). [PubMed: 20132470]

110. Kim HJ et al. A novel mode of TRPML3 regulation by extracytosolic pH absent in the varitint-waddler phenotype. Embo j 27, 1197–1205, doi:10.1038/emboj.2008.56 (2008). [PubMed: 18369318]

111. Grimm C, Jörs S, Guo Z, Obukhov AG & Heller S Constitutive activity of TRPML2 and TRPML3 channels versus activation by low extracellular sodium and small molecules. J Biol Chem 287, 22701–22708, doi:10.1074/jbc.M112.368876 (2012). [PubMed: 22753890]

112. Kim HJ et al. Gain-of-function mutation in TRPML3 causes the mouse Varitint-Waddler phenotype. J Biol Chem 282, 36138–36142, doi:10.1074/jbc.C700190200 (2007). [PubMed: 17962195]

113. Miao Y, Li G, Zhang X, Xu H & Abraham Soman N. A TRP Channel Senses Lysosome Neutralization by Pathogens to Trigger Their Expulsion. Cell 161, 1306–1319, doi:10.1016/j.cell.2015.05.009 (2015). [PubMed: 26027738]

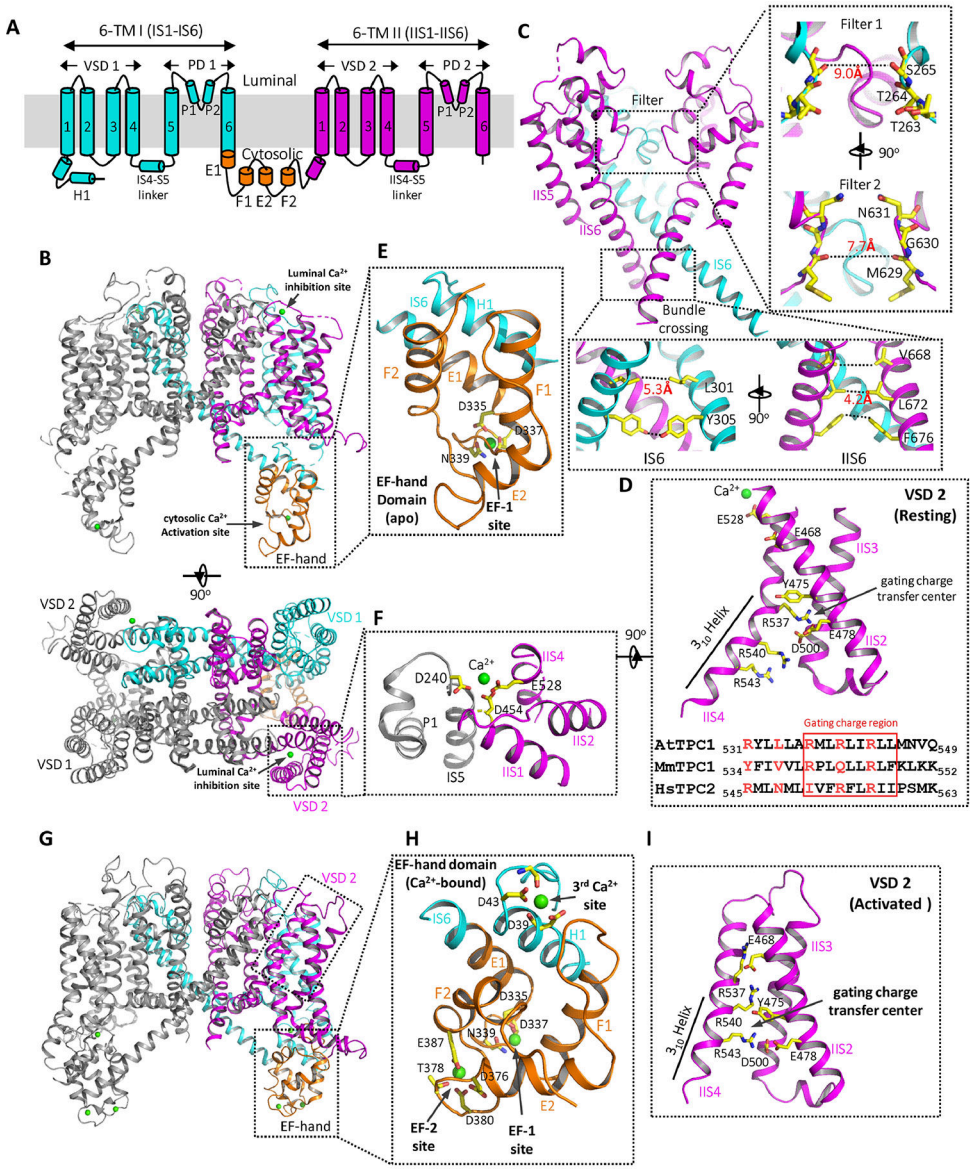

Fig. 1. Structures of AtTPC1.

(A) Topology diagram of one AtTPC1 subunit. [Note: The N-terminal helix that directly interacts with the EF-hand domain was initially labeled as S0 in AtTPC1 but as an H1 helix in mammalian TPCs. To be consistent, it is labeled as H1 in this review.] **(B)** Cartoon representations of the AtTPC1 crystal structure (PDB code: 5E1J)[23]. Domains are individually colored in one subunit as shown in (A) and the other subunit is colored in grey. Ca^{2+} ions are drawn as green spheres. **(C)** Ion conduction pore consisting of IS5–IS6 (PD 1 in cyan with front subunit removed for clarity) and IIS5–IIS6 (PD 2, magenta). Right inset: zoomed-in views of ion pathway at filter 1 and filter 2. Lower inset: zoomed-in views of the bundle crossing formed by IS6 and IIS6 pairs. Numbers are diagonal distances (in Å) at the narrowest constriction points. **(D)** The structure of AtTPC1 VSD2 in the resting state (upper panel with IIS1 removed for clarity) and the partial sequence alignment (lower panel) of IIS4 among AtTPC1, MmTPC1, and HsTPC2. The gating charge region is boxed.

IIS4 is stabilized in a resting state by the luminal Ca^{2+} (green sphere). **(E)** Zoomed-in view of the EF-hand domain with EF-1 in a Ca^{2+}-bound state and EF-2 in an apo state. The two EF-hand motifs are shown in orange; the H1 helix and IS6 are shown in cyan. **(F)** Zoomed-in view of the luminal Ca^{2+} binding site with the Ca^{2+} ion shown as a green sphere. Key residues are colored in yellow. (**G**) The structure of a partially open AtTPC1 (PDB code: 7FHO)[72] with Ca^{2+}-bound EF-hand domain and activated VSD2. (**H**) Zoomed-in view of the Ca^{2+}-activated EF-hand domain with three bound Ca^{2+} ions (green spheres). The F2 helix breaks into two short helices in the Ca^{2+}-bound EF-2 motif. (**I**) zoomed-in view of the activated VSD2 in AtTPC1 with IIS1 removed for clarity.

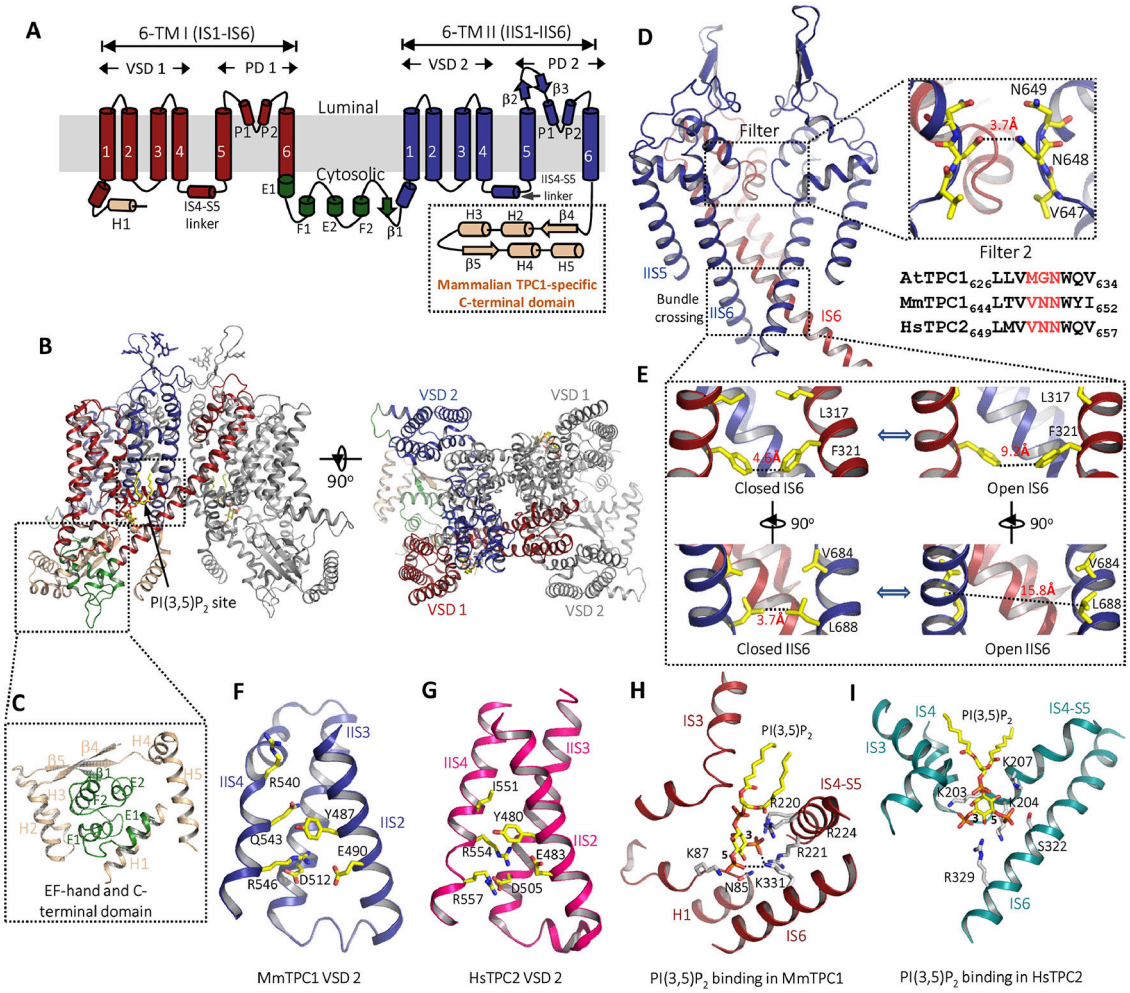

Fig. 2. Structures of mammalian TPCs.

(A) Topology diagram of one MmTPC1 subunit. The C-terminal domain is present in mammalian TPC1 but not TPC2. **(B)** Side and top views of MmTPC1 dimer structure in PI(3,5)P_2-bound open state. Domains in one subunit are individually colored as shown in (A) and the other subunit is colored in grey. PI(3,5)P**2** is shown as yellow sticks. **(C)** Zoomed-in view of MmTPC1 cytosolic soluble region containing the EF-hand domain (green) and the C-terminal domain (salmon). **(D)** MmTPC1 ion conduction pore consisting of IS5–IS6 (PD 1 in red with front subunit removed for clarity) and IIS5–IIS6 (PD 2, blue). Right inset: zoomed-in views of MmTPC1 filter 2 with a partial sequence alignment of filter 2 region among AtTPC1, MmTPC1 and HsTPC2. **(E)** Zoomed-in views of the closed and open cytosolic gates formed by IS6 and IIS6 pairs. Numbers are diagonal distances (in Å) at the narrow constriction points. **(F)** Structure of MmTPC1 VSD 2 with S1 helix removed for clarity. **(G)** Structure of HsTPC2 VSD 2. **(H)** Zoomed-in view of the PI(3,5)P_2 binding site in MmTPC1. **(I)** Zoomed-in view of the PI(3,5)P_2 binding site in HsTPC2. PI(3,5)P_2 is shown in yellow, key residues are shown in white. (PDB codes for the structures used for making the figures are: 6C96 for the apo state MmTPC1; 6C9A for the PI(3,5)P_2 -bound MmTPC1; 6NQ0 for the PI(3,5)P_2 -bound HsTPC2)[25,26]

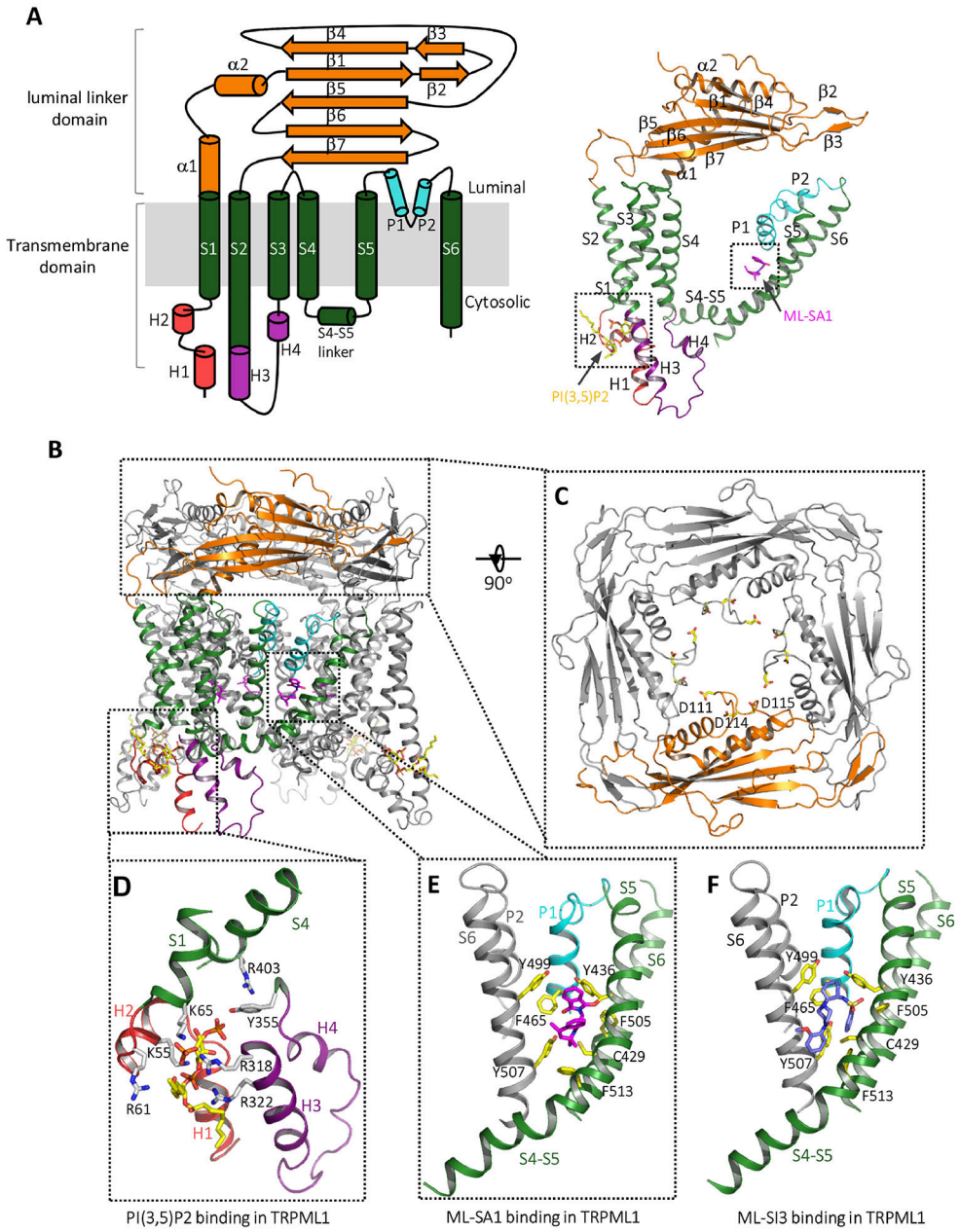

Fig. 3. Structure of mammalian TRPML1.

(A) Topology diagram (left) and the structure (right) of a single HsTRPML1 subunit in the PI(3,5)P_2/ML-SA1-bound open state (PDB code: 6E7Z)[86]. Domains are individually colored. **(B)** The structure of HsTRPML1 homotetramer in the PI(3,5)P_2/ML-SA1-bound open state, one subunit is colored as that shown in **(A)** and the other three are in grey. (**C**) Top view of the luminal linker domain. The three aspartates important for pH-dependent luminal Ca^{2+}-inhibition are shown as yellow sticks. **(D)** The PI(3,5)P_2 binding site in HsTPC1. PI(3,5)P_2 is shown as yellow and red sticks. **(E)** ML-SA1 (magenta) binding site in HsTPC1. **(F)** ML-SI3 (blue) binding site in HsTPC1 (PDB code: 7MGL) [88].